Journal of the Korean Society of Remote Sensing, Vol. 10, No. 2, 1994

A SAR Signal Processing Algorithm using Wavenumber Domain

Joong-Sun Won*, Hong-Ryong Yoo* and Wooil M. Moon**

* Marine Geology Laboratory, Korea Ocean Research and Development Institute

** Department of Geological Science, University of Manitoba

Abstract

Since Seasat SAR mission in 1978, SAR has become one of the most important surface imaging tools in satellite remote sensing. SAR achieves high resolution by signal processing synthesizing a larger aperture. Therefore, SAR signal processing along with antenna technology has been centered upon SAR technologies. Thus interpreters of SAR imagery as well as those who involved in signal processing require the knowledge of the principal SAR processing algorithm. Although the conventional range-Doppler approach has been widely adopted by many SAR processors, azimuth compression including the range migration has been problematic. The recent development of the wavenumber domain approach is able to provide high precision SAR focusing algorithm. Compared with the wavenumber domain algorithm derived by applying Born (first) approximation, the transfer function of the conventional range-Doppler algorithm accounts only for the first order approximation of the exact transfer function. The results of a simulation and an actual test using airborne C-band SAR configuration demonstrate the excellent performance of the wavenumber domain algorithm.

Keyword: SAR, Wavenumber Domain, Focusing

요 약

SAR는 1987년 미국의 인공위성 Seasat에 의해 사용된 이후 현재 그 활용의 중요성이 점차 증대하고 있는 원격탐사 방법중 하나이다. SAR는 특수 신호처리를 통하여 실제 안테나의 길이보다 매우큰 안테나를 사용하는 합성효과를 이용하여 고 해상도를 얻는다. 따라서 안테나 자체의 개발뿐만 아니라 신호처리 기술의 개발이 SAR 기술의 중요한 부분을 차지한다. 따라서 실제 신호처리에 관계자 뿐만아니라 SAR 영상자료를 해석하여 이용하고져하는 사용자들도 SAR 신호처리에 대한 이해가 필요시된다. 비록 rangd-Doppler domain을 이용하는 전통적인 SAR 신호처리 방법이 많이 사용되고 있으나 range

migration과 azimuth compression에서 여러 문제점을 갖고있다. 최근 개발되고 있는 wavenumber domain을 이용한 방법은 좀더 나은 SAR 영상복원을 성취할 수 있는 기반을 마련해 준다. Born (first) 근사법을 이용하여 얻은 새로운 wavenumber domain을 이용한 알고리즘과 비교해볼때 전통적인 방법의 transfer function은 새로운 방법의 일차항까지만으로 이뤄진 근사값이다. 새로운 알고리즘을 이용한 모의실험 및 항공기 c-band SAR로 얻어진 실제 데이터에 적용결과 그 우수성이 판명되었다.

1. Introduction

The synthetic aperture radar (SAR) provides geoscientists with invaluable data of the Earth and planetary surfaces, and has become very important tools in remote sensing techniques. Using microwave signals, SARs are able to image terrestrial surfaces with relative independence of weather and solar illumination conditions. The core techniques of the SAR system are centered on the signal processing as well as improvement of antenna performance, because the SAR achieves high resolution in along- track through a signal processing equivalent to a longer synthetic aperture. The SAR end users as well as those who involved in SAR processing are often required to appreciate the fundamentals of SAR signal processing, because an interpreter could be misled without the knowledge of the SAR processing applied to the SAR image.

An imaging radar system utilizing a synthetic array was developed by C. Wiley in 1952, and initially called "Doppler beam-sharpening system" (Sherwin et al. 1962). An independent experiment with a Doppler processing radar had been conducted by the University of Illinois group in 1953 using an airborne coherent X-band pulsed radar (Brown et al. 1969). The research being developed at the University of Illinois was transferred to the University of Michigan about 1956 (Ulaby et. al. 1981). The first operational SAR system was the Goodyear AN/APQ-102 built for military use, which was operated on X-band (3cm in frequency) with horizontal polarization (Moore 1983). The first public application of SAR survey was carried out for geological mapping in eastern Panama where optic sensors had rarely succeeded in obtaining an imagery because of perpetual cloud cover (MacDonald 1969). The first spaceborne SAR was L-band HH-polarization SAR system on Seasat launched by NASA in 1978 (Jordan 1980). A series of spaceborne SAR missions have been planned and carried out through 1980's and 1990's after the Seasat. The chronology of spaceborne SAR system is summarized in Table 1.

In the SAR signal processing terms, the "focusing" refers to a phase correction of a synthetic aperture array. The SAR focusing had been achieved by optical processing

similar to holographic technique till early 1980's. Although optical SAR processing are rarely performed currently, the frame works of SAR signal processing has been established during the early stage of SAR developments. Excellent references regarding optical SAR processing can be found in a collection of papers, Synthetic Aperture Radar (Kovaly ed. 1976). As the capability of computer systems has been remarkably improved during last decades, digital SAR processing techniques have become popular. Early works on digital SAR processing are described in Brown et.al.(1969), Kirk(1975), and Martinson(1975). However, a full-scale processing scheme had not been materialized until Wu(1976), van de Lindt(1977), and Bennett and Cumming(1979). The principal strategy of these algorithms is based upon chirp technique using two sequential one-dimensional correlations; the range correlation first, range migration correction in the range-Doppler domain, and then azimuth correlation. We will call algorithms adopting above processing sequence "conventional SAR processing approach (or Range-Doppler domain approach)" in the following.

Table 1. Chronology of spaceborne SAR systems (Li and Raney 1991).

Launch Date	Mission	Country
July 1987	SEASAT	U.S.A.
November 1981	SIR-A	U.S.A.
September 1983	Kosmos-1500 (RAR)	U.S.S.R.
October 1984	SIR-B	U.S.A.
July 1987	Kosmos-1870 (AlmaZ I)	U.S.S.R.
August 1990	MAGELLAN	U.S.A.
March 1991	Almaz II	U.S.S.R.
July 1991	ERS-1	Europe
February 1992	JERS-1	Japan
Spring 1994	SIR-C/X-SAR	U.S.A.
1994 (?)	ERS-1	Europe
1995 (?)	RADARSAT	Canada
1996 (?)	CASSINI/TITAN	U.S.A.

Details and difficulties of the conventional SAR processor are reviewed in Barber(1985). Recently Rocca et al.(1989) developed a new SAR processing approach utilizing wavenumber domain (or f-k domain). At similar time but independently Raney and Vachon(1989) also developed a phase preserving SAR processor by exploiting phase shifting in the wavenumber domain. This paper is focused on a SAR processing algorithm using wavenumber domain, which derived directly from the wave equation and Born (first)

approximation for SAR focusing. We are able to achieve the exact transfer function of SAR point scatterer through this approach.

In the next section, theoretical background of the general SAR processing and the wavenumber domain algorithm is described. Simulation and test results are discussed in the third section followed by conclusions and discussions in the last section.

2. Theoretical Background

The heart of SAR technology is the SAR processing technique which enable a short antenna to be synthesized into a longer antenna, and consequently high resolution in along-track or azimuth dimension. Chirp technique (or matched filtering) is commonly used for range compression, and is also utilized for azimuth compression in conventional SAR processors. However, discussion about the chirp technique is beyond the scope of this paper. The reader interested in the details of chirp technique may refer to Cook and Bernfeld(1967).

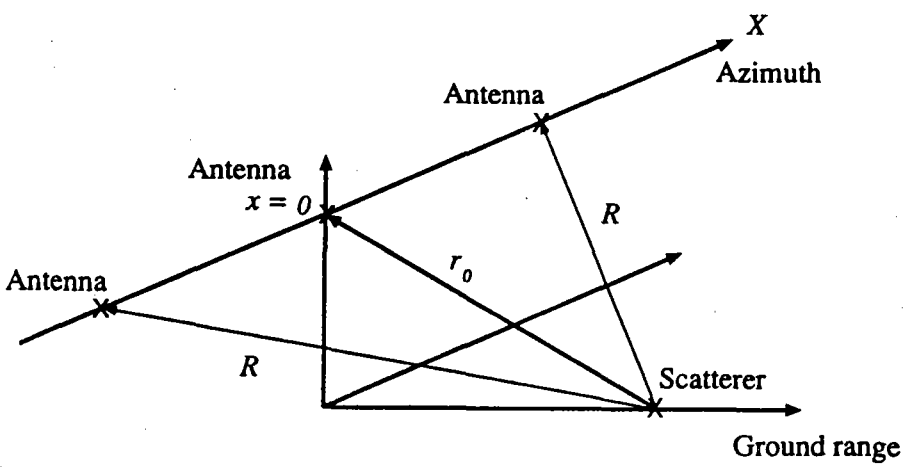

Figure 1. Sensor and a point scatterer geometry.

Figure 1. shows a sensor and a point scatterer geometry. In SAR data space, the response function of a pointer scatterer (so called point scatterer response) is smeared out into two-dimensional function. The SAR processing tries to focus the point scatterer response back to a single point. Therefore, it is important to understand the behaviour of a

point scatterer response. When a pulse transmitted by a antenna is given by

$$p(t)\exp\{-i\omega_0 2R/c\} \tag{1}$$

where $\omega 0$ is the carrier angular frequency, then the echo from the scatterer after range compression can be written as

$$\delta(t-2R/c)\exp\{-i2\omega_0 R/c\} \tag{2}$$

where λ is wavelength and δ is delta function. As Figure 1 shows, the range R can be approximated as

$$R(x;r_0)=\sqrt{r_0^2+x^2}\simeq r_0+\frac{x^2}{2}r_0 \tag{3}$$

Using this quadratic approximation of range in Eq.(3), the point scatterer response function can be approximated as

$$s(x,t;r)=\delta\left(t-\frac{2}{c}r-\frac{x^2}{cr}\right)\exp\left\{-i\omega_0\frac{2}{c}\left(r+\frac{x^2}{2r}\right)\right\} \tag{4}$$

The second exponential term represents the Doppler phase shift, and the range migration can be expressed by

$$\begin{aligned}\Delta R(x;r) &= R(x;r)-r=\sqrt{r^2+x^2}-r\\ &\simeq x^2/2r\end{aligned} \tag{5}$$

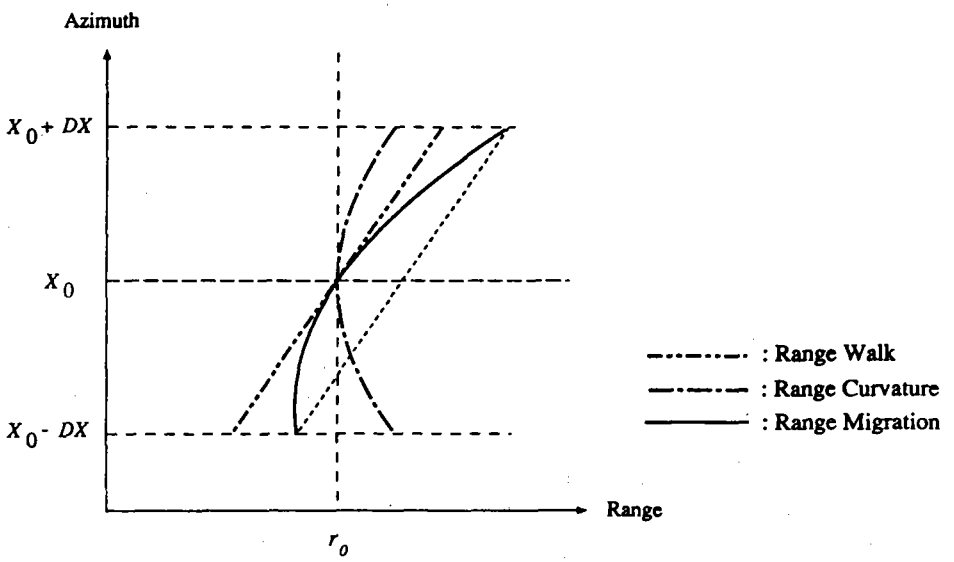

Figure 2. Range curvature, range walk, and range migration.

The trajectory of range curvature in Eq.(5) is as shown in Figure 2, and makes SAR processing two-dimensional problem. Conventional approaches perform the range migration correction and azimuth compression in the range-Doppler domain based upon quadratic approximation in Eq.(4). In order to obtain the point scatterer response in the range-Doppler domain, we can take the Fourier transform with respect to azimuth x resulting in

$$s(k_x, t; r) \sim \sqrt{i\frac{\lambda r}{2}}\, e^{-i4\pi r/\lambda}\, \delta\left(t - \frac{2}{c} r - \frac{cr}{4}\frac{k_x^2}{\omega_0^2}\right) \exp\left\{i\frac{cr}{4}\frac{k_x^2}{\omega_0}\right\} \tag{6}$$

where k_x is the azimuth wavenumber or spatial angular Doppler frequency. The range migration correction in the range-Doppler domain is carried out as time shift by

$$\Delta t(k_x) = -\frac{cr}{4}\frac{k_x^2}{\omega_0^2} \tag{7}$$

This range migration correction step requires a certain interpolation in range, which is often difficult to achieve with high accuracy. After the range migration correction a one-dimensional transfer function (complex conjugate of the point scatterer response) is applied for azimuth compression such as

$$\exp\left\{-i\frac{cr}{4}\frac{k_x^2}{\omega_0}\right\} \tag{8}$$

This rang-Doppler domain algorithm has been developed by Wu(1976), Bennett and Cumming(1979), and van de Lindt(1977). However, this approach only accounts for up to the first order approximations of ω/ω_0 as we will discuss end of this section.

A SAR processing algorithm using wavenumber domain can be achieved by applying Born (first) approximation to the wave equation. The Helmholtz equation is given by

$$\left(\nabla^2 + \frac{\omega^2}{c^2}\right) s(r, r_o; \omega) = -f(r - r_o) \tag{9}$$

where $s(r, r_o; \omega)$ is the total field, and f is the source function. Antenna coordinate r_o and the scatterer coordinate r is as shown in Figure 3.

The total field can be decomposed into the incident field s_i and the scattered field s_s, and therefore the total field can be written as

$$s(r, r_o; \omega) = s_i(r, r_o; \omega) + s_s(r, r_o; \omega) \tag{10}$$

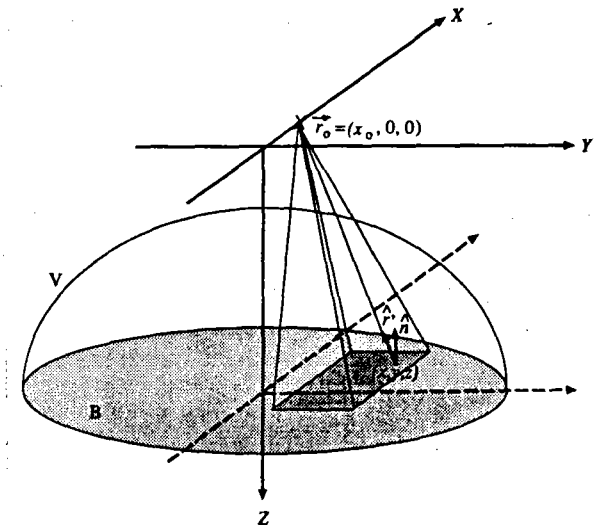

Figure 3. Schematic diagram of the SAR geometry and integration volume of Green's integral.

Substituting Eq.(10) into Eq.(9) and integrating over the volume V in Figure 3, we have non-linear equation. If surface scattering is dominant, we can assume that (Won and Moon 1992)

$$\begin{aligned} s_s(r, r_o; \omega) &\sim \sigma(r) s_i(r, r_o; \omega) \\ \frac{\partial}{\partial n} s_s(r, r_o; \omega) &\sim \sigma(r) \frac{\partial}{\partial n} s_i(r, r_o; \omega) \end{aligned} \tag{11}$$

This approximation corresponds to the Kirchoff boundary condition in optics (Goodman 1968), and this condition is similar to Born (first) approximation for this problem (Won and Moon 1992). Using Eq.(11), we have final inversion formula given by

$$\begin{aligned} \sigma(x, r') \sim A \int\int \sqrt{\frac{k_r}{k_r^2 + k_x^2}}\, e^{i r_0 (k_r + \sqrt{k_r^2 + k_x^2})} \\ \Theta\left(k_x; \frac{c}{2}\sqrt{k_r^2 + k_x^2}\right) e^{i(k_x x + k_r r')} dk_x dk_r \end{aligned} \tag{12}$$

where

$$\Theta \equiv \omega \frac{\partial}{\partial \omega}\left(\frac{s_s(x_0, 0, 0; \omega)}{\omega}\right) \tag{13}$$

and $r' = r - r_0$ where r_0 is the minimum slant range, and A is a constant. Derivation of Eq.(12) from Eq.(9) is described in detail by Won and Moon(1992), and

Won(1993). Eq.(12) is two-dimensional inverse Fourier transform of Θ, and therefore SAR image can be focused using wavenumber domain processing and simple two-dimensional Fourier transform. The proposed processing steps are summarized by a flow chart in Figure 4.

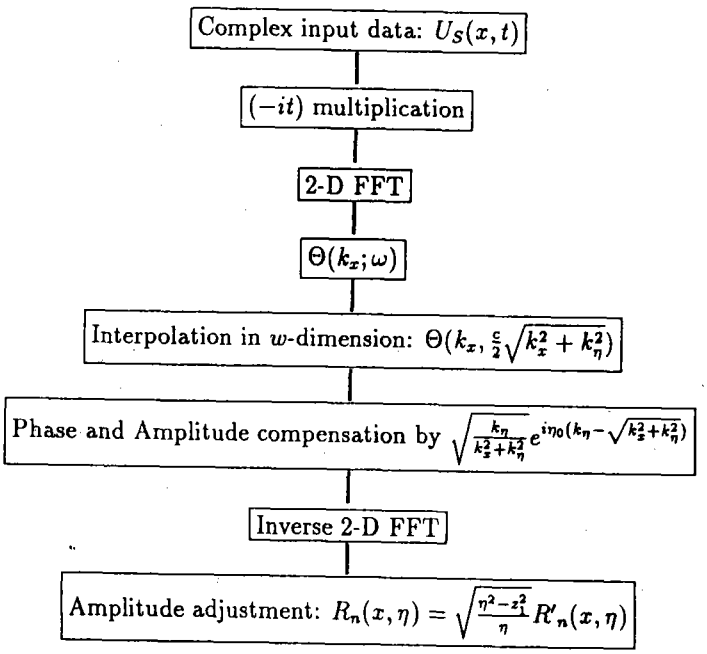

Figure 4. Flow chart of the proposed wavenumer domain algorithm.

Eq.(12) can be further approximated to be

$$\sigma(x,r') \sim A\int\int \left[\left(\frac{\omega+\omega_0}{c/2}\right)^2 - k_x^2 \right]^{-1/4} \Theta(k_x;\omega)\, e^{i(xk_x+2r'\omega/c)} \exp\left\{ ir\left[\sqrt{\left(\frac{\omega+\omega_0}{c/2}\right)^2 - k_x^2} - \frac{\omega+\omega_0}{c/2} \right] \right\} dk_x d\omega \tag{14}$$

Using Eq.(14) and Eqs.(7) and (8), we can make a comparison of the range-Doppler approach and this wavenumber domain approach. Eqs.(7) and (8) used in the conventional approach correspond to the last exponential term in Eq.(14) which is derived directly from wave equation and thus exact formula. Because the range migration correction of Eq.(7) is equivalent to phase shift in wavenumber domain, the combined two-dimensional transfer function of Eq.(7) and (8) is given by

$$\exp\left\{-ir\frac{c}{4}\frac{k_x^2}{\omega_0^2}(\omega_0-\omega)\right\} \tag{15}$$

and the exact transfer function in Eq.(14) corresponding to Eq.(15) can be approximated as

$$\exp\left\{ir\left[\sqrt{\left(\frac{\omega+\omega_0}{c/2}\right)^2-k_x^2}-\frac{\omega+\omega_0}{c/2}\right]\right\} \simeq \exp\left\{-ir\frac{c}{4}\frac{k_x^2}{\omega+\omega_0}\right\} \tag{16}$$

because $(\omega_0+\omega)^2 \gg (ck_x/2)^2$ for most SAR systems. Now we can see Eq.(15) used in the range-Doppler approach is an approximation of the exact transfer function in Eq.(16) only up to the first order of ω/ω_0. An improvement was made in order to accommodate large range migration by Jin and Wu (1984).

3. Simulation and Test Results

A simulation is carried out in order to test the performance of the wavenumber domain algorithm. The CCRS C-band airborne SAR system parameters (narrow swath mode) are used for the simulation. Specifications of the CCRS C-band airborne SAR system (Livingstone et.al. 1988) is summarized in Table 2, and its operating geometries are shown in Figure 5.

Table 2 Specifications of CCRS's C-band airborne SAR system (Livingstone et al. 1988)

	Narrow Swath	Wide Swath
Transmitter		
Nominal altitude	6 Km	
Frequency	5.3 GHz	
Wavelength	5.66 cm	
PRF/Velo	2.32 or 2.57 Hz/m/s	
Chirp length	7 μm	8 μm
Receiver		
Compressed pulse width	40 ns	120 ns
Noise figure	5.2 dB	3.7 dB
Antenna	3.0 deg.	
Azimuth beamwidth	4.2 deg.	29 deg.
Elevation beamwidth	20 deg.	22 dB
Peak gain	24 dB	
Resolution		
Azimuth	6 m	10 m
Range	6 m	20 m

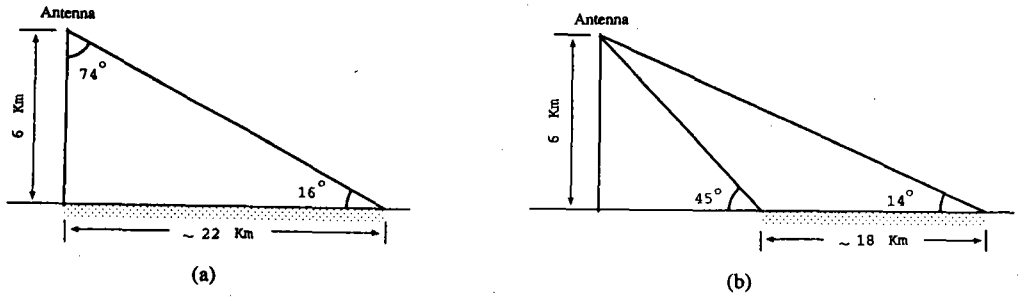

Figure 5. CCRS's airbornr SAR operating geometries: (a) the nadir mode, (b) the narrow swath mode.

SAR signals of 1024 by 1024 data array are simulated first using a point scatterer with unit backscattering coefficient. The SAR signals can be simulated through a two-dimensional convolution as described by Wu et al. (1982). After range compression the simulated input signal is as shown in Figure 6 (a). In Figure 6, the range and azimuth sampling interval are respectively 4 m and 0.39 m, and thus the azimuth dimension is exaggerated by about ten times. The point scatterer is reconstructed by applying the wavenumber domain algorithm (see Figure 4) as shown in Figure 6 (b). The 3 dB width in azimuth of the focused point scatterer is about 2.8 m. Because the required azimuth resolution is 6 m, this simulation result demonstrates excellent performance of the wavenumber domain algorithm.

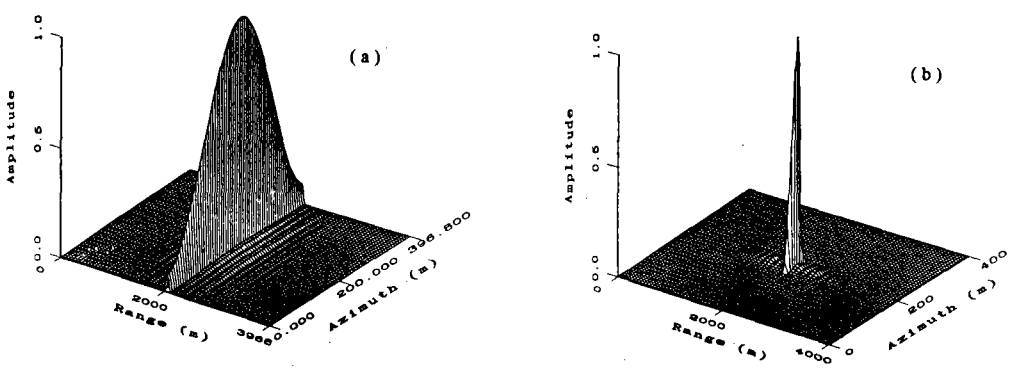

Figure 6. Airborne simulation: (a) a simulated signal of 1024 by 1024 data array, and (b) the reconstructed amplitude image. The range and azimuth sampling interval are re spectively 4 m and 0.39 m.

A test has been carried out using CCRS's airborne C-band SAR data acquired over Ottawa, Canada. As shown in Figure 5 (a), the test data was acquired in the nadir half swath mode with C-band (5.67 cm) HH-polarization. The average altitude and platform velocity are respectively 6 Km and 134.76 m/sec. The pulse repetition frequency is 343 Hz, and thus the ratio of the pulse repetition frequency to the platform velocity is 2.57 (1/m).

Figure 7. Raw SAR signal image acquired over Ottawa airport, Canada, using CCRS's C-band SAR system. Flight direction is from top left to top right in the image.

Figure 8. Reconstructed image by applying the wavenumber domain algorithm. Flight direction is from top left to top right in the image.

The slant range and azimuth sampling interval are about 4 m and 0.39 m, respectively. In this nadir mode, the receiving antenna is turned on about 13.2 μsec before the first arrival of the echo signal, and that would include the nadir line as a part of image. The image of 2048 (raw) by 8192 (azimuth) signal data array is shown in Figure 7. The I/Q signal data is converted to amplitude data and quantized into a 8 bits data. A linear histogram stretching is applied to produce the image in Figure 7. A bright azimuth line at near range represents the nadir line in Figure 7. The wavenumver domain algorithm summarized in Figure 4 is applied to obtain the focused image in Figure 8. Amplitude of the processed image is interpolated in the azimuth dimension in order to produce square pixel. In the processed image in Figure 8, structures such as runways and other roads are very well focused. Surface characteristics of this SAR image are roughly divided into two

Figure 9. A close-look image of far range area in Figure 8.

area: the near range area where agricultural areas are dominant; and the far range area where urban structures are dominant. Figure 9 is a close-look image of urban area in Figure 8. Structures of white cross hair line correspond to corner scatterers such as high building. In order to evaluate the performance of the algorithm, the 3 dB azimuth width of a point scatterer is measured to be about 4.1 m. Although this 3 dB width (4.1 m) is bigger than that of simulation result (2.8 m in narrow swath mode), it is till good enough to be fitted into one required resolution (6 m).

In short, the simulation and actual test results demonstrate the performance of the wavenumber domain approach even though the inversion technique is still in the early developing stage. However, ceratin details of the implementation of the wavenumber domain approaches are yet to be quantitatively investigated and tested.

4. Conclusions and Discussions

A SAR inversion formula in the wavenumber domain has been established based upon the Born (first) approximation concept, in which the incident field as well as the backscattered field is included in this approach. The inversion formula is derived directly from the wave equation, and therefore this approach provides the exact transfer function. The transfer function commonly used in conventional range-Doppler algorithms accounts only for the first approximation of the transfer function in the wavenumber domain approach.

The simulation results demonstrate the performance of the proposed algorithm accommodating the range curvature. The processing results applied to the CCRS's airborne C-band SAR data acquired in nadir mode turned out to be slightly less focused than the simulation results (narrow swath mode) in terms of 3 dB azimuth width. However, the 3 dB azimuth width in the processed airborne SAR image is smaller than the required azimuth resolution. Although simulation and actual test results demonstrate the performance of the wavenumber domain approach, quantitative assessments of the algorithm using satellite-borne SAR system data are required to verify specifically phase preservation capability of the algorithm.

Recently, a new approach of SAR processing using chirp scaling has been developed by Runge and Bamler (1992), and Raney (1992). These algorithms based on chirp scaling completely replace interpolation steps, which has commonly been fundamental obstacles in

most SAR processing algorithms, by phase adjustment. The future works will be focused on the review and sophisticated implementation of the new approach followed by comparison of the algorithm utilizing chirp scaling and the wavenumber approach discussed in this paper.

Acknowledgements

This research is financially supported by the Korean Ocean Research and Development Institute to J.S. Won (BSPE 00432-664-5). The airborne C-band SAR data was provided by CCRS.

References

Barber, B.C., 1985, Theory of digital imaging from orbital synthetic-aperture radar, *Int. J. Remote Sensing*, 6-7: 1009-1057.

Bennett, J.R. and Cumming, I.G., 1979, Digital SAR image formation airborne and satellite r esults, *Proc. 13th Int'l Symp. Remote Sensing Environ.*, pp. 168-175.

Brown, W.M. and Porcello, L.J., 1969, An introduction to Synthetic Aperture Radar, *IEEE Spectrum*, September, pp. 52-62.

Cook, C.E. and Bernfeld, M., 1967, *Radar Signals: An Introduction to Theory and Applicati on,* Academic Press.

Goodman, J.W., 1968, *Introduction to Fourier Optics,* McGraw-Hill Book Co., pp. 37-42.

Jin, M.Y., and Wu, C., 1984, A SAR correlation algorithm which accommodates large-range migration, *IEEE Trans. Geosci. Remote Sensing*, 22-6: 592-597.

Jordan, R.L., 1980, The Seasat-A synthetic aperture radar system, *IEEE J. Ocean Eng.*, vol. 5, pp. 154-164.

Kirk, J.C. Jr., 1975, A discussion of digital processing in synthetic aperture radar, *IEEE Tr ans. Aerosp. Electron. Syst.*, 11-3: 326-337.

Kovaly, J.J.(ed.), 1976, *Synthetic Aperture Radar,* Artech House, Inc., 335p.

Li, F.K. and Raney, R.K., 1991, The special section on spaceborne radars for Earth and pla netary observations, *Proc. IEEE*, 79-6: 773-775.

van de Lindt, W.J., 1977, Digital technique for generating synthetic aperture radar images, *IBM J. Res. Develop.*, September, pp. 415-432.

Livingstone, C.E., Gray, A.L., Hawkins, R.K., and Olsen, R.B., 1988, CCRS C/X-band airbor ne synthetic aperture radar: An R and D tool for the ERS-1 time frame, *IEEE Aero sp. Electron. Syst. Magazine*, October, pp. 11-16.

MacDonald, H.C., 1969, Geologic evaluation of radar imagery from Darien Province, Panam a, *Modern Geol.*, vol. 1, pp. 1-63.

Martinson, L., 1975, A programmable digital processor for airborne radar, *Proc. IEEE Int. Radar Conf.*, pp. 186-191.

Moore, R.K., 1983, *Imaging radar systems: Manual of Remote Sensing, 2nd ed.* (R.N. Col well ed.), American Society of Photogrammetry, pp. 429-474.

Raney, R.K., Vachon, P.W., 1989, A phase preserving SAR processor, *Proc. IGARSS '89*, pp. 2588-2591.

Raney, R.K., 1992, An exact wide field digital imaging algorithm, *Int'l J. Remote Sensing*, 13-5: 991-998.

Rocca, F., Cafforio, C., and Prati, C., 1989, Synthetic aperture radar:A new application for wave equation techniques, *Geophysical Prosepecting*, vol. 37, pp. 809-830.

Runge, H. and Bamler, R., 1992, A novel high precision SAR focussing algorithm based on chirp scaling, *Proc. IGARSS '92*, pp. 372-375.

Sherwin, C.W., Ruina, J.P., and Rawcliffe, D., 1962, Some early developments in Synthetic Aperture Radar systems, *IRE Trans. Military Electron*, 6-2: 111-115.

Ulaby, F.T., Moore, R.K., and Fung, A.K., 1981, *Microwave Remote Sensing Active and P assive*, Addison-Wesley, vol. I, pp. 5-12.

Won, J.S. and Moon, W.M., 1992, Inversion of synthetic aperture radar for surface scatterin g, *Geophys. J. Int.*, vol. 108, pp. 423-432.

Won, J.S., 1993, Inversion of Synthetic Aperture Radar (SAR) Data using Born Approximat ion and SAR Image Enhancement for Geological Application, Ph.D. Thesis (University of Manitoba), pp. 64-84.

Wu, C., 1976, A digital system to produce imagery from SAR data, *Proc. AIAA Syst. Desi gn Driver by Sensors*, Paper 76-968.

Wu, C., Liu, K.Y., and Jin, M., 1982, Modeling and a correlation algorithm for spaceborne S AR signals, *IEEE Trans. Aerosp. Electron. Syst.*, vol. 18, pp. 563-574.